Contract Information

Contract Number	HR0011-05-1-0031
Title of Research	Nanodevices from Nanocomponents: Memory, Logic and Mechanical Nanodevices
Principal Investigator	Dr. Charles J. O'Connor
Organization	University of New Orleans, New Orleans, LA 70148

FINAL TECHNICAL REPORT – May 11, 2009

Purpose:

The purpose of this report is to document the results of the complete effort for this project, which was to investigate the development of nanodevices from nanoscale components. The project focused on exploring the possibilities of employing nanoparticles and other nanocomponents to fabricate nanodevices. The four main components of the project were: quantum dot memory devices, multilevel logic devices, electromechanical devices, and nanosensor devices.

Progress Summary:

(1) Quantum Dot Memory Devices (Jiye Fang, Charles J. O'Connor, and Leonard Spinu)

This component of the program focused on the development of high quality Ge nanoparticles (germanium quantum dots) for applications in nonvolatile flash memory devices. Our initial goal for this component of the project was to pursue three areas of the research: (1) synthesis of Ge NCs through a high-temperature organic solution strategy; (2) assembly of Ge NCs and deposition of the pattern onto SiO_2 matrix using Langmuir-Blodgett technique; (3) evaluation of the new feature of this Ge NC nonvolatile memory based on high-frequency capacitance-voltage (C-V) and current-voltage (I-V) measurements. However, due to the devastating effects of Hurricane Katrina, which hit New Orleans just short of four months after the project began, the lead co-PI, Dr. Jiye Fang, left the University of New Orleans, and this area of research was discontinued for the project. This is a summary of the research in this component which was completed during the first year of the project.

Research Progress:

Our initial efforts were directed at the synthesis and preparation of germanium (Ge) nanocrystals (NCs) as the principal nanocomponent for further development for use as a floating gate device in nonvolatile flash memory. This material was chosen because of its known narrow bandgap and its special electron affinity, which is similar to that of silicon (Si). The synthetic approach which we pursued was in two directions: (1) to create a synthetic route for producing high-quality Ge NCs, and to explore a processing technique of embedding these Ge Ncs into

SiO2; and (2) to explore the encapsulation of semiconductor Ge quantum dots into the orderly arrays of mesopores.

Strategy of Synthesis (1): In this approach, we focused our research efforts on two areas: to create a synthetic route of producing high-quality Ge NCs, and to explore a processing technique of embedding these Ge Ncs into SiO2. We have conducted the synthesis of Ge NCs through an improved reduction process by employing a high-temperature organic solution approach in non-polar system. This investigation could be broken down to three sections: (1) test of reaction agents; (2) optimization of reaction conditions; (3) characterization of products. Meanwhile, we have also explored an alternative processing route, one-pot synthesis of Ge nanoparticles embedded into an ordered mesoporous material, in order to achieve the target material by one-step.

Results (1): (a) Testing of Reaction agents: We have realized that the following commercially available chemicals could be used as candidates of Ge precursors: $GeCl_4$ (mp: –49.5 °C, bp: 89.1 °C.); $GeBr_4$ (mp: 26.1 °C, bp: 186.5 °C.); GeO_2 (mp: 1086 °C); GeI_4 (mp: 146 °C) and Ge ethoxide. We chose $GeBr_4$ as our first Ge-precursor simply because of its boiling point (bp), which was consistent with our high-temperature solution-synthesis approach. The disadvantage of using this compound lies on its high cost (about $200 per 10g). We initially utilized superhydride as the reducing agent. However, our experiments indicated that this expensive organic reducing agent could be replaced by using $NaBH_4$ in our system, as long as an emulsion was formed assisted by an ultrosonication before the injection of the reducing agent-solvent suspension into the hot solution system containing Ge precursor.

(b) Typical reaction and optimized parameters: Non-polar solvent benzyl ether was selected as our high-temperature reaction medium. A proper amount of oleic acid was tentatively employed as the capping agent. In a typical experiment, 0.1 mL of GeBr4 was added into 10ml benzyl ether in the presence of 1 mL of oleic acid. The vigorously stirred mixture was heated to certain temperature in a three-neck flask equipped with a condenser under an argon stream. Excess amount of $NaBH_4$ suspension in benzyl ether (4-5 mL) was then injected into the flask at this high-temperature and the subsequent reaction was maintained and the products were separated and purified as what described elsewhere.

Based on our experimental results, we realize that relatively low reaction temperature favor the formation of Ge NCs. In different experiments, the reaction temperature was varied from 120 to 270 °C. When the reaction temperature was maintained at around 200 °C, well-crystallized Ge NCs could be achieved; whereas increase of the temperature to 200 °C would result in a barrier of collecting the Ge component from the products. The XRD pattern of our products, showed that Ge NCs existed as a major phase, as all of the detectable peaks from this XRD pattern can be indexed as those of Ge based on the standard ICDD PDF card. By applying the Scherrer equation to the line broadening of several typical peaks, the average crystalline size was estimated as ~ 8 nm in size.

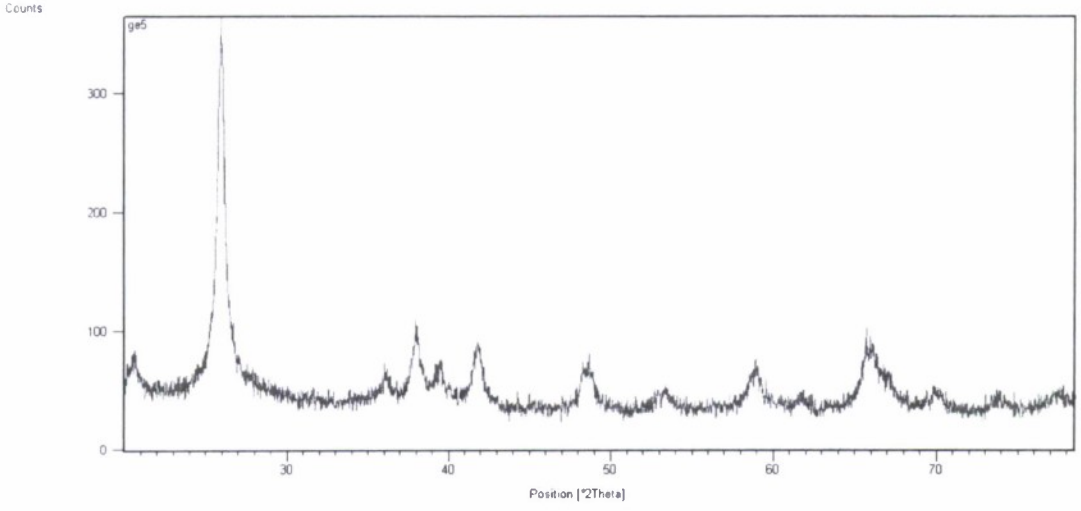

Fig.1 XRD trace of Ge NCs prepared at 200 °C

The XRD trace determined on the product synthesized at 270 °C under the same experimental conditions suggested that NaBr as a major component dominates such product obtained at 270 °C. The difference of products due to two different reaction temperatures requires further investigation.

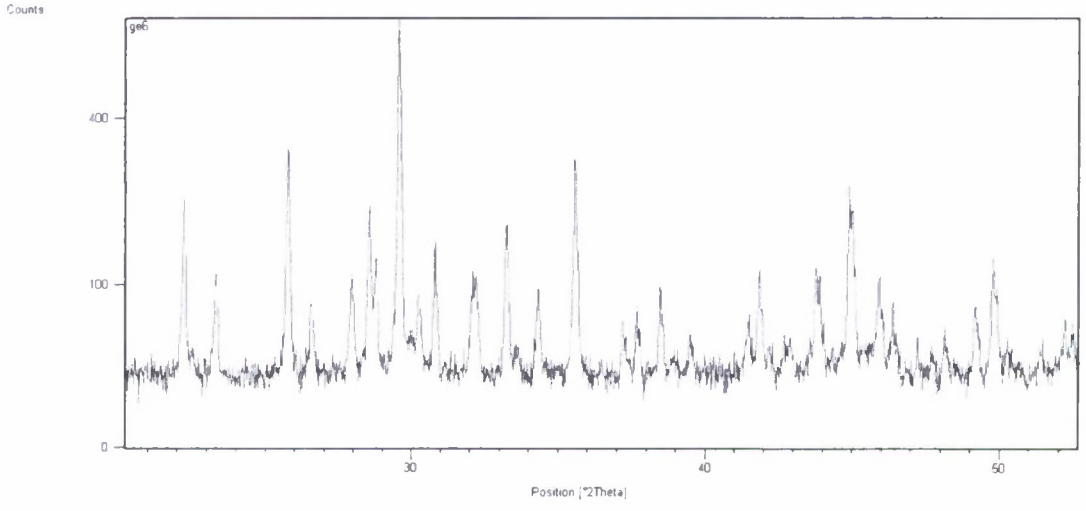

Fig.2 XRD trace of the as-prepared product at 270 °C. Analysis implies that NaBr is a major component in this product.

(c) Alternative Exploration on Synthesis of SiO_2-coated nanoparticles: In this exploration, we used monodisperse PbSe NCs as example, and successfully developed a coating technique. Typical TEM images are shown below, demonstrating a novel processing pathway of producing SiO_2-coated nanoparticle). We will replace PbSe NCs with Ge NCs in our future study.

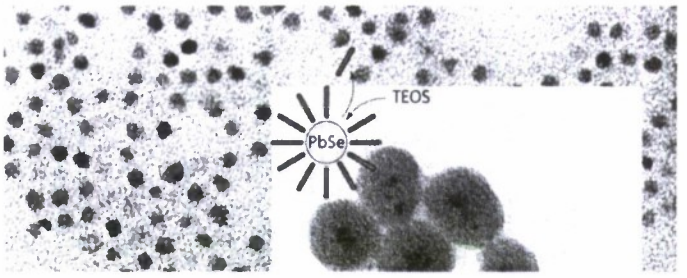

The synthesis approach of PbSe NCs is based on a procedure previously developed. The PbSe@SiO_2 particles were prepared by a modified W/O microemulsion method at room temperature. The microemulsion system was made up of cyclohexane, NP-5, PbSe and dimethylamine. Typically, 10 ml cyclohexane, 1.3 ml NP-5, 400 μl PbSe stock-solution (8.72×10^{-7} mol/L) and 50 μl TEOS (99.999 %) were added in a glass container under vigorous stirring. 30 min after the microemulsion system was formed, 100 μl dimethylamine aqueous solution (40wt %) was introduced to initiate the polymerization process. Following the reaction, the first evidence for silica-encapsulation is provided by the colour of the precipitate containing the composites, which are typical for specific NCs and their sizes and the disappearance of that colour from the solution by an increase of light-scattering. The silica growth was completed after 24 h of stirring. The nanoparticles were destabilized from the microemulsion using acetone and precipitated by centrifugation. The resultant precipitate of PbSe@SiO_2 composite particles was washed in sequence with 1-butanol, 1-propanol, ethanol and water to remove any possible surfactant and unreacted molecules. For each washing step, followed by centrifugation, a sonicator bath was used to completely disperse the precipitate in the corresponding solvent and remove any physically adsorbed molecules from the particle surfaces. Finally, aqueous dispersions of the composite particles were obtained.

Strategy of Synthesis (2): In order to encapsulate semiconductor Ge quantum dots in the orderly arrays of mesopores, (1) we prepared the highly ordered mesoporous MCM-41 with columnar periodic hexagonal pores with diameter of 3-4 nm. We also systematically investigated the morphologies of mesostructured silica under various experimental conditions, and developed a procedure of fabricating relatively large MCM-41 crystal. (2) We have then introduced germanium tetrabromide into these calcined MCM-41 silica crystals by using a vacuum system, followed by a posttreatment.

Various characterizations on these Ge-impregnated MCM-41 silica crystals were undertaken. (3) Further surface treatment will include precision ion polishing process in which, the surface of MCM-41 will be cut off, and additional I-V, C-V evaluations on each Ge-point in a MCM-41 sample. These steps are illustrated in a cartoon scheme below:

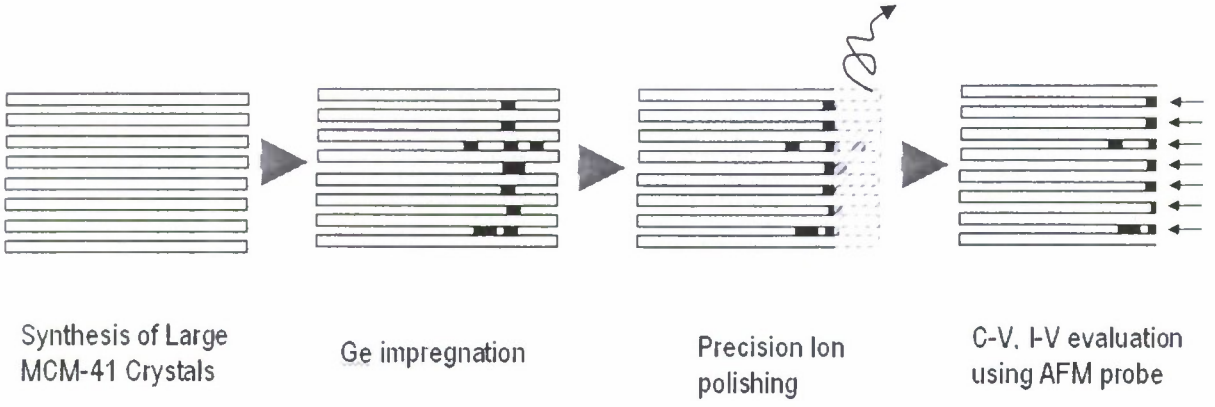

Results (2): (a) Synthesis of large-size MCM-41 crystals. Typical syntheses of ordered MCM-41 silica crystals were typically carried out by slowly introducing TEOS into NH_4OH solution in the presence of CTAB as surfactant. The product was then filtered, washed and dried at ambient temperature, followed by calcination in air at 823 K for 4 h. We further optimized a number of parameters including synthetic temperature, pH value, concentration of TEOS and surfactant ratio to refine the size of MCM-41 crystals. The size of MCM-41 crystal could be varied from submicro to 10 micrometer. The morphology and microstructure of a typical sample are shown in Figure 1.

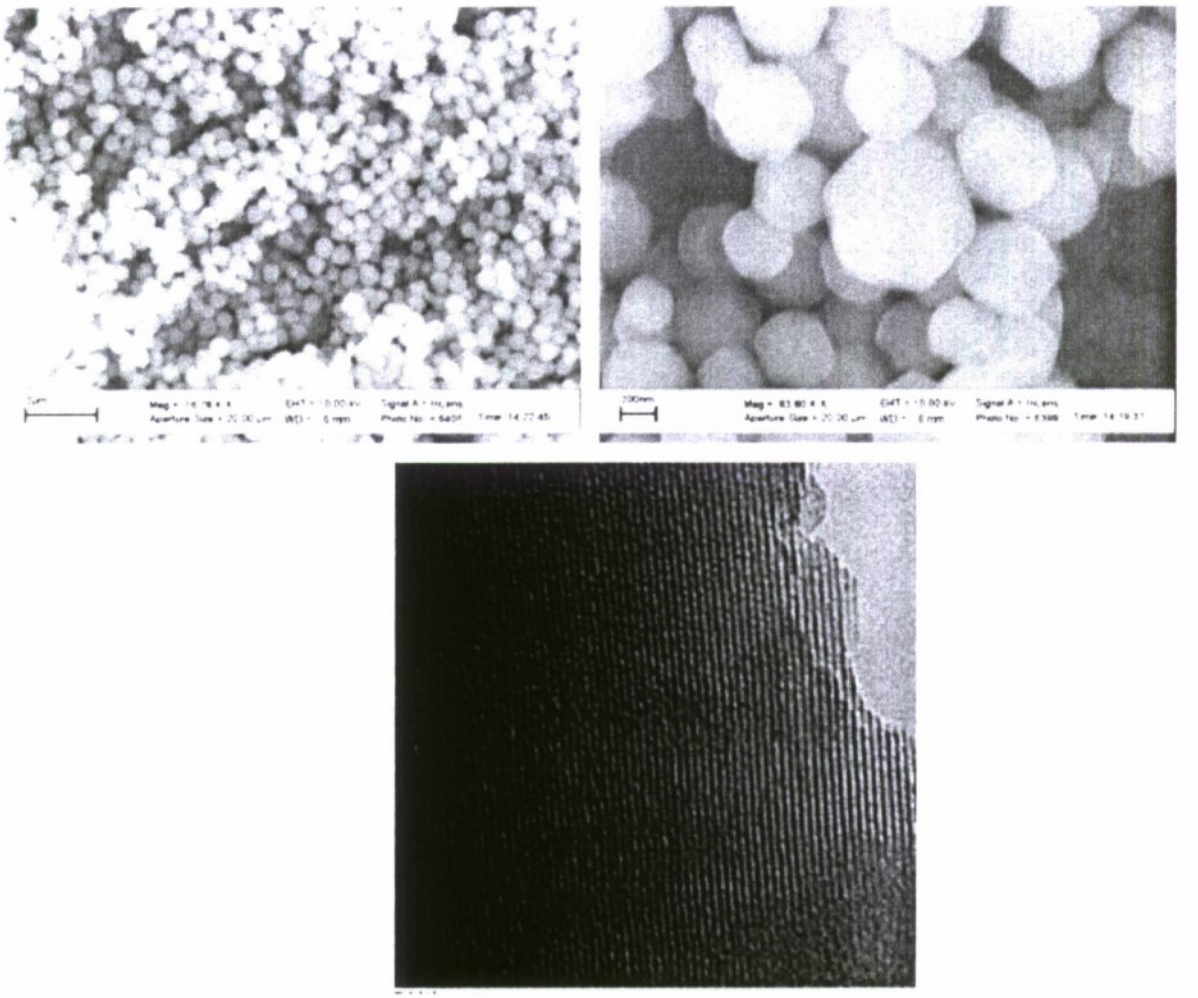

Figure. 1, (a) low magnification SEM image of highly ordered MCM-41 silica particles; (b) high magnification SEM of the MCM-41 particles (c) HRTEM images of the MCM-41 particle.

(b) Pore filling with Ge. We have then impregnated THF solution of germanium tetrabromide into these calcined MCM-41 silica crystals by operating a vacuum system. The impregnation was repeated after evaporation of the solvent. After the solvent was completely removed under vacuum, the MCM-41 sample impregnated with $GeBr_4$ was mounted inside a quartz container and heated to 100 ^{0}C under H_2 flow for 12h, and to 250 ^{0}C for 4h. The sample was subsequently annealed at 500 ^{0}C for 2h. The calcination process can get ride of hydroxyls on the inner channel surfaces of the MCM-41 matrix as well as other chemical species. Meanwhile, at high temperature with H2 flow $GeBr_4$ is reduced into metallic Ge which remains inside the MCM-41 channels. Sufficient times of Ge-precursor loading leads to a condensation and pore filling with Ge. By control of the impregnation times of germanium tetrabromide, however, it is very possible to form discrete Ge dots with high crystallinity in the channels rather than continuous wires. Figure 2 is TEM images showing MCM-41 channels with filled Ge. The further structure-characterizations are still being in progress.

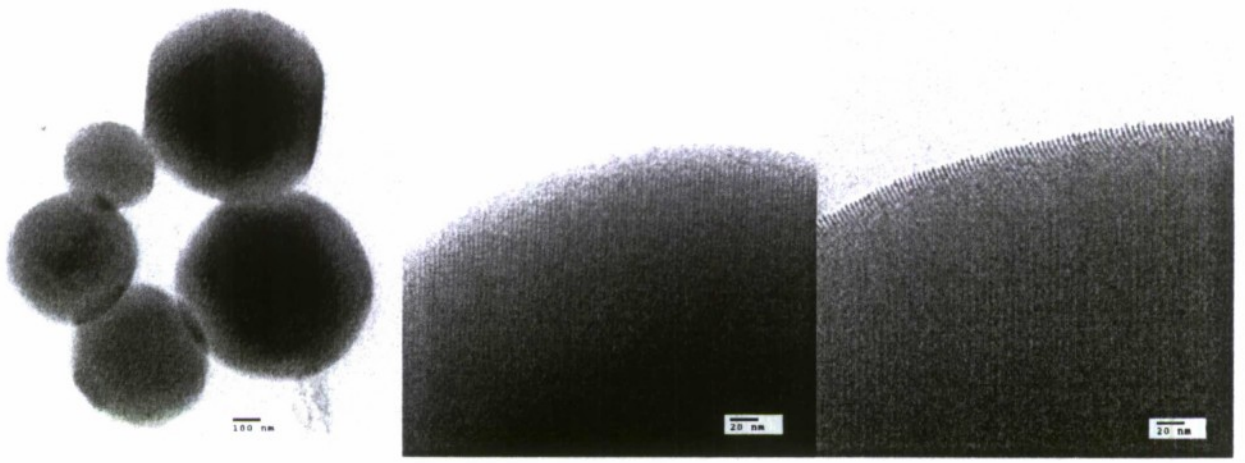

Figure 2: TEM images showing the structures of MCM-41 Matrixes where Ge has been introduced.

\

Conclusions: (1) It is a feasible to prepare Ge NCs by following the route we suggested in our project proposal. (2) There is a challenge of controlling and refining the GE NC morphology. In other words, we need to continuously investigate/test various potential chemicals and to select more efficient molecule as the capping agent. (3) It has attracted our attention to achieve the designed materials by one-pot synthesis of Ge nanoparticles embedded into an ordered mesoporous SiO2.

Publications:

Formation of PbSe Nanocrystals: A Growth toward Nanocubes, Weigang Lu, Jiye Fang, Yong Ding and Zhong Lin Wang, *J. Phys. Chem. B,* 109, 19219-19222 (2005).

Low-Temperature Anomalies of the Two-Photon Absorption in In_2O_3 Nanocrystals Incorporated into PMMA Matrixes, I. V. Kityk, Qingsheng Liu, Zhaoyong Sun and Jiye Fang, *J. Phys. Chem. B,* 110(16), 8219-8222 (2006).

Silica Encapsulation of Hydrophobically Ligated PbSe Nanocrystals, Masih Darbandi, Weigang Lu, Jiye Fang and Thomas Nann, *Langmuir*, 22 (9), 4371- 4375 (2006).

Drastic Increase of the Second-Order Susceptibilities for Monodisperse In_2O_3 Nanocrystals Incorporated into PMMA Matrices, I. V. Kityk, J. Ebothé, Qingsheng Liu, Zhaoyong Sun and Jiye Fang, *NanoTechnology*, 17(8), 1871-1877 (2006).

Syntheses of Ag, PbSe and PbTe Nanocrystals and Their Binary Self-Assembly Exploration at Low Size-ratio, Weigang Lu, Jiye Fang, Jun Lin, Jun Zhang, Zhaoyong Sun and Kevin L. Stokes, *J. NanoSci. NanoTechno.*, 6(6), 1662-1666 (2006).

Presentations:

"Synthesis, Characterization and Evolution Mechanism Study of Chalcogenide and Oxide Nanocrystals", Jiye Fang, the 13th National Science Foundation Workshop on Materials Chemistry & NanoScience, invited & sponsored by NSF, October 28-31, 2005, Alexandria, Virginia.

"Progress in Synthesis of Functional Nanocrystals", Jiye Fang, State Key Laboratory of Rare Earth Chemistry and Physics, Changchun Institute of Applied Chemistry, Chinese Academy of Science, Changchun, P.R. China, July 13, 2005.

(2) Multilevel Logic with Magnetic Nanosized Building Blocks (Leonard Spinu, Weilie Zhou, and John B. Wiley)

Research Progress:

We proposed a new method for a synthetic antiferromagnet (SAF) structure's critical curve (CC) determination. This study is motivated by the fact that knowing the magnetic anisotropy of SAF structures is essential for the devices like magnetic random access memories (MRAM). The method is based on reversible susceptibility's singularities detection as the magnetic field is swept along easy axis, in both positive and negative direction, while a hard axis bias field is also applied. By performing susceptibility measurements with different values of the bias field, CC can be determined (see Fig. 1). It is shown that this method can reveal the entire CC for both low and high values of the exchange coupling. Susceptibility measurements are currently performed in order to study the SAF's critical curves, using the proposed method.

We have studied the dynamic switching of SAF elements from MRAM memories and its dependence on thermal effects. The model is based on LLG and SLLG equations, which are numerically integrated. The magnetic layers are assumed to be ellipsoid shaped with each magnetic layer single domain. Simulations were performed for both balanced and non-balanced SAF elements. The switching properties are discussed as a function of applied field pulses length and shape. We have shown that besides non-switching, toggle and direct write mode1, an inverse write mode can be identified. In dealing with the problem of improving the writing time, one needs to pay careful attention to the parameters describing the pulses shape. As the applied field sweep rate rises, the switching diagrams increasingly have layer-like structures with switching/non-switching areas (see Fig. 2).

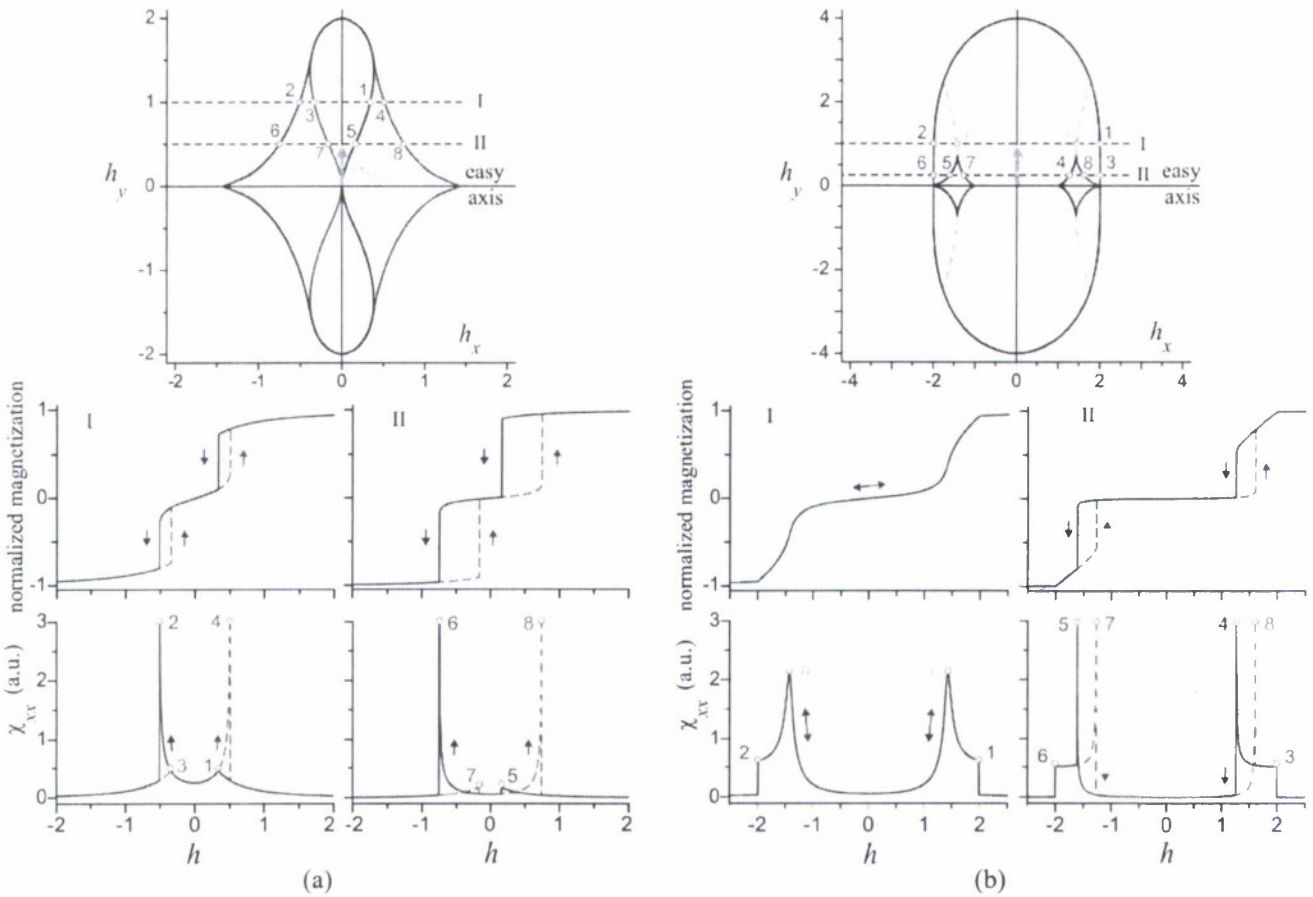

FIG. 1. (a) Critical curve (top) for a symetric SAF structure with an exchange coupling $h_J = 0.5$, as the magnetic field is swept along easy axis, in both positive and negative direction, while a hard axis bias field is also applied. Middle: the projection of the normalized magnetic moment on the sweeping field's direction. (b) Same as (a), but with exchange coupling $h_J = 1.5$.

This alternating behavior has two causes: the ringing of the magnetization during the field and the layer-like structure of basins of attraction of fixed points. A reliable switching is obtained only if the ringing is avoided either by a precise control of a pulse and MRAM cell parameters so that the system moves along a ballistic trajectory, or using a relatively slow rise time pulse. Also, we have presented how the thermal fluctuations affect the switching behavior.

Recently, the current-induced spin-transfer torque has been proposed as a convenient writing process in high density magnetic random access memory. A spin-polarized current can switch the magnetization of a ferromagnetic layer more efficiently than a current induced magnetic field. Based on the magnetization vector dynamics, as described by LLG/SLLG equation of motion, the switching properties of a spin-valve type tri-layer structure have been investigated. We have shown that in the switching diagrams the boundary which delimits the stable switching and non-switching regions is not smooth, having a layer-like structure (fringes), the switching and non-switching areas alternating with

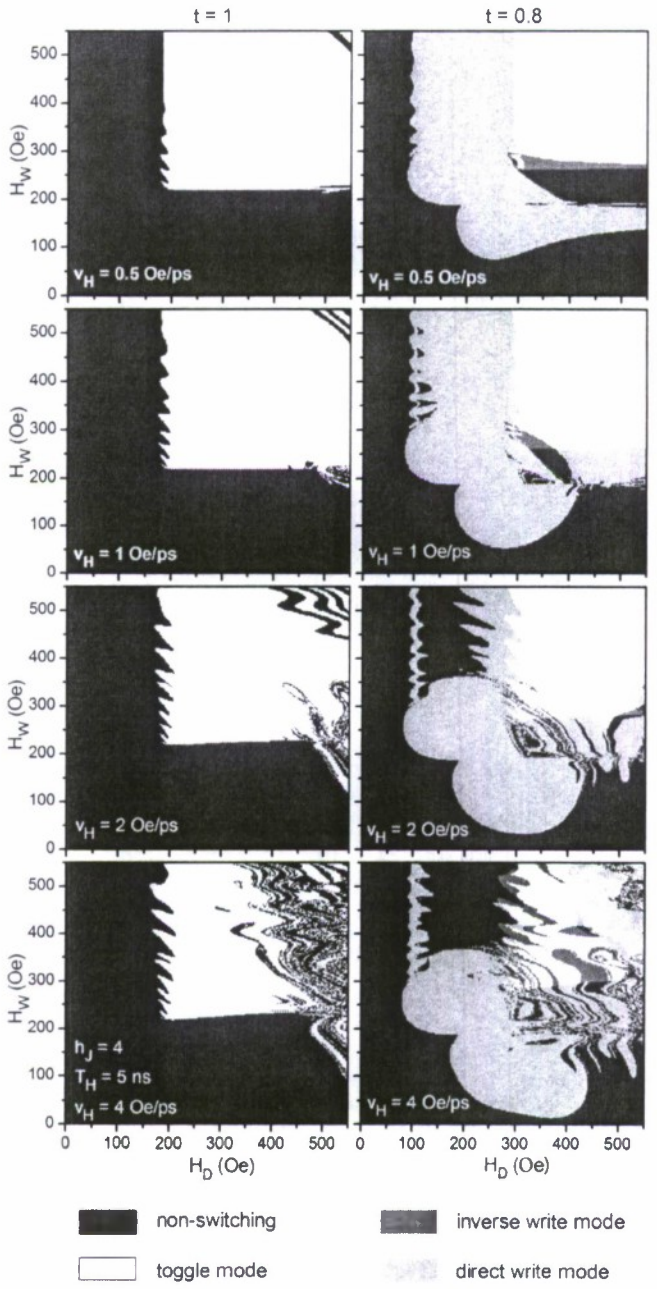

FIG. 2. Switching diagram of a balanced (left) and a non-balanced (right) SAF element at $T = 0\,\mathrm{K}$, as a function of the applied field pulse strengths.

increasing current pulse amplitude and duration. These fringes exist when the current is cut-off and evolves in time into a more intricate structure. When the pulse's length is too short, a significant ringing of the magnetization still exists during the current pulse and the final state is determined by the position of the magnetization at the end of the pulse. For a fast and reliable switching such ringing must be avoided, as the damping time can take several nanoseconds. The ringing may be diminished, for example, using a relatively slow rise time pulse. Also, we have presented how the thermal fluctuations affect the switching behavior.

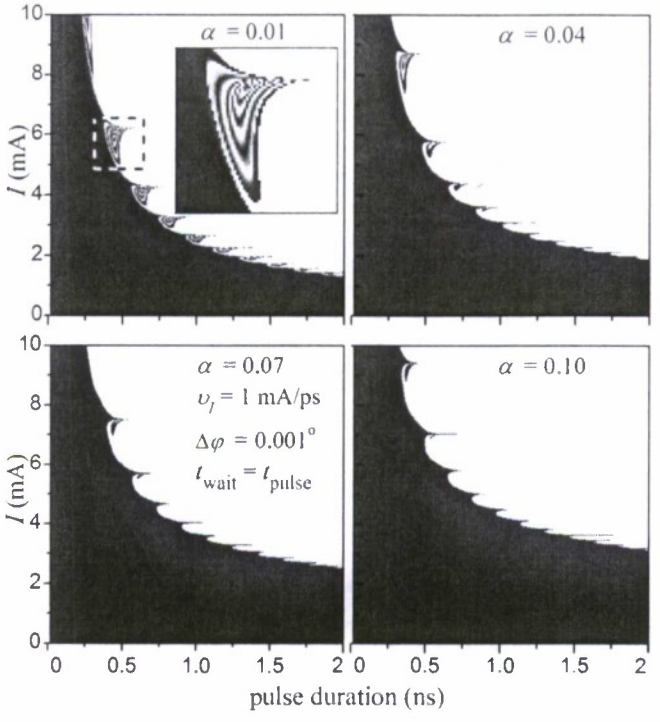

FIG. 3. Antiparallel-parallel switching diagrams at $T = 0$ K, as a function of current pulse amplitude and duration, for a current sweep rate $\upsilon_I = 1$ mA/ps, and different values of damping constant α. Black areas represent $m_x = -1$ (where m_x is the **m**'s projection on the x axis), white areas represent $m_x = 1$, and the intermediate values of m_x are represented with shades of gray. The state of the magnetic moment is taken after a time equal with the pulse duration, after the pulse's termination. The inset (top left) shows a zooming into a portion of the border between stable switching and non-switching zones.

Publications:

C. Radu, D. Cimpoesu, A. Stancu, and L. Spinu, "Measurement of the critical curve of a synthetic antiferromagnet," Appl. Phys. Lett., vol. 93, p. 3, Jul 2008.

D. Cimpoesu, L. Spinu, and A. Stancu, "Transverse susceptibility method in nanoparticulate magnetic media," J. Nanosci. Nanotechnol., vol. 8, pp. 2731-2744, Jun 2008.

D. Cimpoesu, A. Stancu, L. Spinu "Dynamic and temperature effects in toggle magnetic random access memory" J. Appl. Phys. 102(1), 013915-1-7 (2007)

Dorin Cimpoesu, Alexandru Stancu, and Leonard Spinu, "Physics of complex transverse susceptibility of magnetic particulate systems," *Phys. Rev. B.*, vol. 76, pp. 054409, 2007.

Dorin Cimpoesu, Alexandru Stancu, and Leonard Spinu, "Dynamic and Temperature Effects in Toggle Magnetic Random Access Memory," *J. Appl. Phys.*, vol. 102, pp. 013915, 2007.

Dorin Cimpoesu, Alexandru Stancu, and Leonard Spinu, "The Reversible Susceptibility Tensor of Synthetic Antiferromagnets," *J. Appl. Phys.*, vol. 101, pp. 09D112, 2007.

Cosmin Radu, Dorin Cimpoesu, Erol Girt, Ganping Ju, Alexandru Stancu, and Leonard Spinu," Reversible Susceptibility Studies of Magnetization Switching in FeCoB Synthetic Antiferromagets," *J. Appl. Phys.*, vol. 101, pp. 09D109, 2007.

Dorin Cimpoesu, Alexandru Stancu and Leonard Spinu, "Micromagnetic Study of the Complex Transverse Susceptibility of Uniaxial Ferromagnets with Quartic Anisotropy," *IEEE Trans. Magn.*, vol. 43, pp. 2905-2907, June 2007.

Presentations:

D. Cimpoesu, A. Stancu, L. Spinu, *"Complex transverse susceptibility in magnetic particulate media,"* 6th International Symposium on Hysteresis Modeling and Micromagnetics HMM-2007, Naples, Italy, June 4-6.

D. Cimpoesu, A. Stancu, and L. Spinu, *"Dynamic and Temperature Effects in Toggle Magnetic Random Access Memory,"* Poster presentation at the 10th Joint MMM/Intermag Conference, Baltimore, MD, January 7-11 2007.

D. Cimpoesu, A. Stancu and L. Spinu, *"The Reversible Susceptibility Tensor of Synthetic Antiferromagnets,"* Poster presentation at the 10th Joint MMM/Intermag Conference, Baltimore, MD, January 7-11 2007.

C. Radu, D. Cimpocsu, E. Girt, G. Ju, A. Stancu, and L. Spinu, *"Reversible Susceptibility Studies of Magnetization Switching in FeCoB Synthetic Antiferromagets,"* Poster presentation at the 10th Joint MMM/Intermag Conference, Baltimore, MD, January 7-11 2007.

D. Cimpoesu, A. Stancu and L. Spinu, *"Micromagnetic Study of the Complex Transverse Susceptibility of Uniaxial Ferromagnets with Quartic Anisotropy,"* Poster presentation at the 10th Joint MMM/Intermag Conference, Baltimore, MD, January 7-11 2007.

Dorin Cimpoesu, Alexandru Stancu and Leonard Spinu, *"Complex Transverse Susceptibility in Magnetic Particulate Media,"* Poster presentation at the 6th International Hysteresis Modeling and Micromagnetics Symposium, Naples Italy, June 4- June 6 2007

Leonard Spinu, *"Theory and Experiment of Complex Transverse Susceptibility,"* Invited talk at the IEEE ROMSC Conference, Iasi Romania, May 26 – May 29 2007

(3) Electromechanical devices (John B. Wiley, Weilie Zhou, Bruce Gibb, and LeonardSpinu)

Research Progress:

This program focuses on the controlled assembly of nano-objects into complex nano-systems. The general approach involves the development of hosts (H1, H2 and H3 (Figure 1)) that bind complementary guests (G1, G2 and G3). Each host-guest pair is orthogonal, i.e. H1-G1 associates, but for example H1-G2 or H3-G1 do not. Hence, a surface of a nano-object coated with H1 will stick to another coated with G1. Moreover, with three, orthogonal host-guest pairs, it is theoretically possible to assemble complex objects by selectively coating different objects (or different parts of objects) with different hosts and guests. Our strategy is to utilize thioether-functionalized deep-cavity cavitands (DCC) and complementary guests that bind to gold surfaces. Our work to date is detailed below.

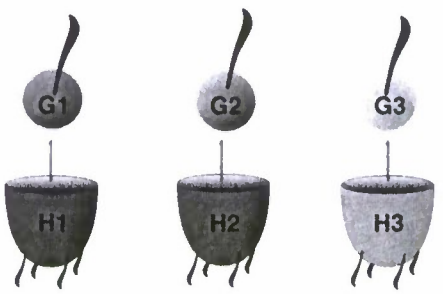

Figure 1

The synthetic strategy chosen was adapted from a report by Reinhoudt.[1] Of importance is the choice of thioether feet for the DCC (e.g., **4**) over thiols. Reinhoudt has reported better surface coverage is obtained using thioether feet as they are able to fold back under the head group upon binding of the sulphur atom to the gold surface to more effectively pack the space under the receptor. This results in a densely packed, more organized monolayer that passivates the gold surface better.[2]

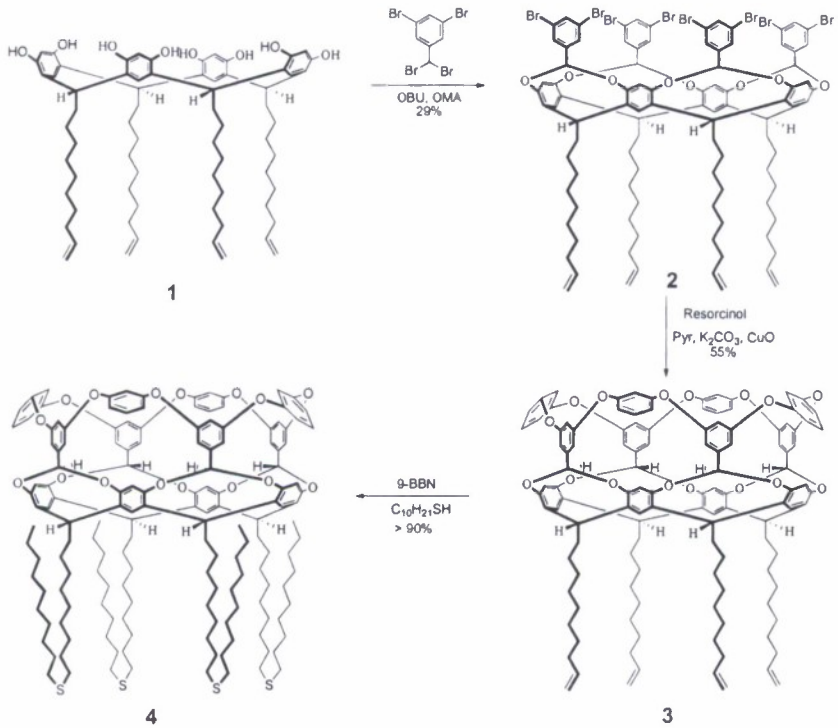

Scheme 1: Synthesis of host **4**

The syntheses of the three hosts are illustrated by the synthesis of the first example, host **4**, shown in Scheme 1. Briefly, known **1** is treated with 3,5-dibromobenzal bromide to yield cavitand **2**. An eight-fold Ullmann ether reaction using four equivalents of resorcinol subsequently yielded DCC **3**, which upon reaction decanethiol in the presence of 9-BBN gave the target **4**. By similar methods, hosts **5** and **6** have also been synthesized.

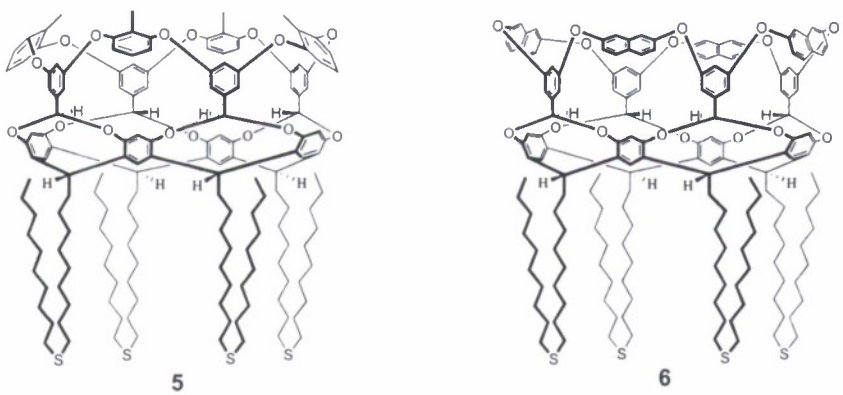

Our route to guests complementary to hosts **4** and **5** is outlined in Scheme 2. Briefly, amide bond formation between the corresponding acids and amines gave **7** and **8** respectively. Subsequent reaction with potassium thioacetate yielded the thioesters **9** and **10**, hydrolysis of which gave targets **11** and **12**. From previous results, we anticipated that the adamantyl guest **11** would bind to host **4**, whilst guest **12** would bind to host **5**. Additionally, we anticipated that **11** would be too large to bind to **5**, while **12** would be too small to strongly associate with **4**.

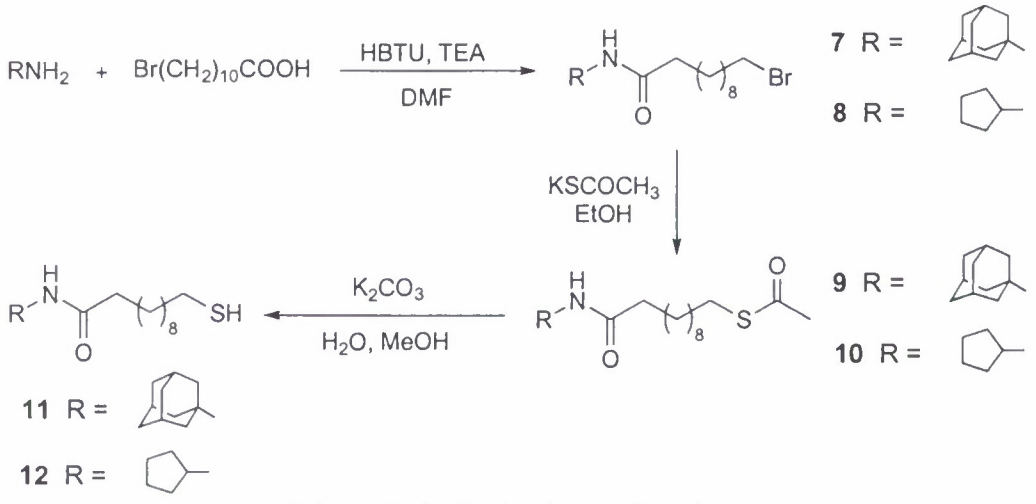

Scheme 2: Synthesis of guests **11** and **12.**

We have used NMR to measure the association constants of guests **11** and **12** binding to their complementary hosts **4** and **5**. The association between **4** and **11** was measured at 95 M^{-1}, a relatively weak interaction on its own, but one that is ideal for multi-valancy interactions between two nano-objects coated with many copies of each. In contrast, we detected no interaction between **5** and **12**. The analogous results that this host-guest pair was based on involved a guest possessing a bromine atom that we knew significantly increased binding strength. We are therefore currently synthesizing a guest similar to **12** but possessing a bromine atom in the 3-position of the five-membered ring. We anticipate this guest will engender our second suitable host-guest pair. Future studies will examine the synthesis of a third host-guest pair.

References:

1. E.U. Thoden van Velzen, J.F.J. Engbersen, P.J. de Lange, J.W.G. Mahy and D.N. Reinhoudt *J. Am. Chem. Soc.* **1995**, 117, 6853-6862.
2. E.U. Thoden van Velzen, J.F.J. Engbersen and D.N. Reinhoudt *Synthesis* **1995**, 989-997.
3. E. Menozzi, R. Pinalli, E.A. Speets, B. Jan Ravoo, E. Dalcanale and D.N. Reinhoudt *Chem. Eur. J.* **2004**, 2199-2206.

Presentations:

Bruce C. Gibb and Melissa J. Latter, *"Deep Cavity Cavitands,"* **2006**, 232nd American Chemical Society National Meeting; San Francisco, California.

(4) Nanomaterials for Gas Detection (Weilie Zhou and Charles J. O'Connor)

Research Progress:

A. Non-Aqueous Synthesis of Metal Oxide Nanoparticles and their Nanocomposite Materials

We have developed a novel solution-based method to synthesize several kinds of technologically interesting crystalline metal oxide nanoparticles. In this high-temperature solution-phase process, magnetite (Fe_3O_4), cobalt ferrite ($CoFe_2O_4$), indium oxide (In_2O_3) and lithium cobalt oxide ($LiCoO_2$) nanoparticles have been successfully synthesized and characterizated by transmission electron microscopy (TEM), X-ray diffractometry (XRD), and Superconducting Quantum Interference Device (SQUID) magnetometry. The resulting metal oxide nanoparticles are monodisperse, highly crystalline and they can be easily dispersed in non-polar solvents yielding colloidal solutions which are stable against aggregation for long periods of time. The size of the nanoparticles could be tuned ranging from 4 nm to about 20 nm by using the "seed mediated growth" method. The shape of the nanoparticles could also be controlled from spherical to faceted (diamond and cubic) by altering the type and amount of capping ligands. Also other reaction parameters such as temperature and heating rate were found to affect the particles morphology.

We also synthesized core-shell structure nanocomposites by using some of these nanoparticles as cores with silica, titania or polymer as shells via a modified microemulsion approach. The TEM measurements showed that Fe_3O_4/SiO_2 and In_2O_3/SiO_2 core-shell structure nanocomposites were successfully prepared and the thickness of the silica coating could be controlled from 2 nm to about 100 nm by adjusting the amounts of the reagents used in the micelle system. The SQUID measurements indicate that the magnetic properties of the Fe_3O_4 nanocrystals were minimally influenced by the silica coating. This synthetic approach was extended to the synthesis of core/shell structures containing titania or polymers (PEG and PMMA) as shells. The relationship between the reaction temperature and the aggregation of the core nanoparticles during the coating process was also investigated.

As an effort to develop novel nanomaterials for various technological applications by using simple concepts of colloidal and coordination chemistry we have successfully synthesized various kinds of metal oxide nanoparticles and core/shell structure nanocomposites by combining the thermal decomposition and microemulsion methods.

The resulting nanocrystalline particles are relatively uniform in shape and size and tend to self-assemble in monolayers. The similarity in morphology is critical for the formation of 3D architectures (superlattices) which can be used as building blocks for the design of various nanoscale devices.

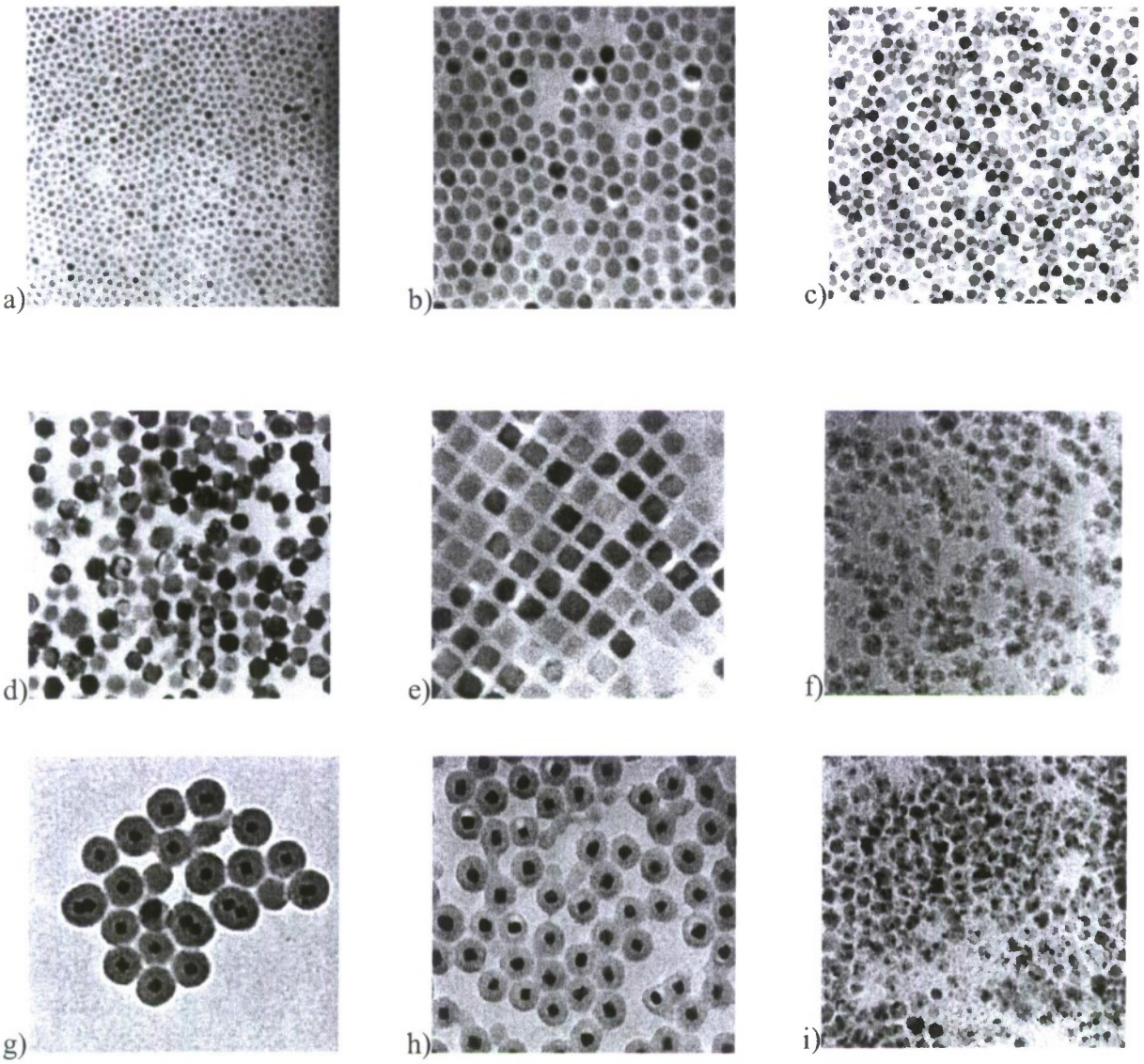

Fig. 1 Bright field TEM images of 8 and 12 nm-sized Fe_3O_4 nanoparticles (a and b); 10 nm (c) and 20 nm In_2O_3 (d) nanoparticles; 10 nm $LiCoO_2$ nanocrystals (e); 8 nm $CoFe_2O_4$ nanoparticles (f) and core-shell nanoarchitectures: 10 nm/2nm Fe_3O_4 /SiO_2 core-shell nanoparticles (g), 10 nm/15nm In_2O_3/SiO_2 core-shell nanoparticles (h) and 6nm/10 nm Fe_3O_4/polystyrene core-shell nanoparticles, respectively

B. Magnetic Measurements of Oxovanadium Organophosphonate Compounds

One interesting class of materials in the studies is the oxovanadium organophosphonates, a structurally diverse family of materials characterized by an increased thermal stability of the V-P-O substructure, readily modified organic substituents and distinct hydrophobic and hydrophilic domains. This structural versatility is reflected in applications to areas as diverse as catalysis,

proton conductivity, ion exchange, intercalation chemistry and photochemistry. Recent research focus has been put on the systematic study of the magnetic properties of these compounds. The magnetic data suggest the mixed valence character of the samples studied and follow the Curie-Weiss law, indicating essentially spin-only magnetism and only very weak intermolecular interactions. One example of the temperature dependence of magnetic susceptibility and effective magnetic moment is shown in Fig. 1.

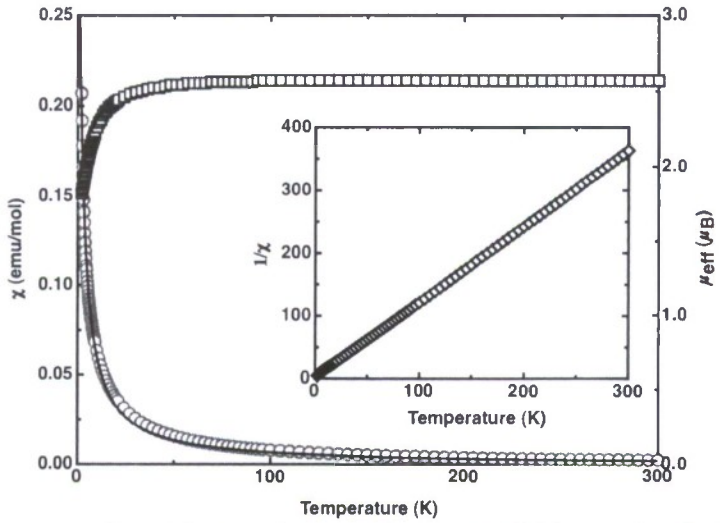

Fig. 1. Temperature dependence of magnetic susceptibility and effective magnetic moment of $[V_3O_3(OH)\{C_6H_3(C_6H_4PO_3H)_3\}] \cdot 7.5H_2O$

These observations of essentially non-interacting V ion sites in these samples are consistent with the magneto-structural correlations for vanadium phosphate phases. The coupling between V ions in these structures depend on the proper orientation of the magnetic orbitals with the in plane oxygen p-orbitals. Thus, the prototypical buttressed layer architecture polyhedral topology of some samples similar to that of $VO(HPO_4) \cdot 4H_2O$ which also exhibits poor transmission of magnetic interactions. Similarly, the strongly axially distorted $\{VO_6\}$ octahedra of the vanadyl chain structure found in other samples would not exhibit significant coupling through the μ-oxo bridges due to the mismatch of the magnetic orbitals.

Publications:

W. Ouellette, G. Wang, H. Liu, G.T. Yee, C.J. O'Connor, and J. Zubieta, "The Hydrothermal and Structural Chemistry of Oxovanadium-Arylphosphonate Networks and Frameworks," *Inorg. Chem.*, 48(3), 953-963 (2009).

Y.-H. Chuang, H. Liu, C.J. O'Connor, and J. Zubieta, "Organic-Inorganic Hybrid Oxides: Structure and Magnetic Properties of $[\{Cu(terpy)\}_2Mo_6O_{17}(H_2O)(O_3PCH_2NH_2CH_2PO_3)_2]\cdot H_2O$, a Bimetallic Oxide Constructed from Novel $\{Mo_6O_{17}(H_2O)(O_3PCH_2NH_2CH_2PO_3)_2\}_4$- Clusters," *Inorg. Chem. Commun.*, 11(10), 1205-1208 (2008).

Zhang, M.; Cushing, B. L.; O'Connor, C. J., "Synthesis and Characterization of Monodisperse Ultra-Thin Silica-Coated Magnetic Nanoparticles," *Nanotechnol.*, *19*, 085601 (2008).

J.J. Liu, K. Wang, M.H. Yu, and W.L. Zhou "Room Temperature Ferromagnetism of Mn Doped ZnO Align Nanowire Arrays with Temperature Dependent Growth" J. Appl. Phys., 102, 024301D (2007).

J. J. Chen, Y. Yan, A. West, J. J. Liu, and W. L. Zhou "Characterization of Diluted Magnetic Semiconductors of Co-doped and (FeCo)-codoped ZnO Nanostrutures by Nanoprobe EDS Analysis" Microscopy & Microanalysis, 13 (Supp.) 737CD (2007)

J.J. Liu, M.H. Yu, and W.L. Zhou, "Fabrication of Mn Doped ZnO Diluted Magnetic Semiconductor Nanostructures by Chemical Vapor Deposition," J. Appl. Phys., 99, 08M119/1-08M119/3 (2006).

Presentations:

Kai Wang, Jiajun Chen, and Weilie Zhou, "Synthesis and Magnetic Properties of In2-xNixO3 Nanowires," Res. Soc. Fall Meeting, Nov.26 - Nov.30, 2007, Boston, MA.

K. Wang, J. Chen, and W. Zhou, "Synthesis of Fe-doped and FeCu-codoped Zinc Oxide Nanowire Arrays for Spintronic Applications," poster presentation, DARPA UNO AMRI Review and Symposium, New Orleans, LA, February 15-16, 2007.

J. Chen and W. Zhou, "Spintronic Devices Based on One-Dimensional Metal Oxide Semiconductors," poster presentation, DARPA UNO AMRI Review and Symposium, New Orleans, LA, February 15-16, 2007.

O.D. Fregene, J. Chen, and W. Zhou, "Fabrication of Pure and Doped TiO2 Nanoparticles and SnO Nanowires by Physical Vapor Deposition Method for Spintronics," poster presentation, DARPA UNO AMRI Review and Symposium, New Orleans, LA, February 15-16, 2007.

J. Zhou, J. Chen, and W.L. Zhou, "Individual and Multiple ZnO Nanowire Nanosensors for Sensitive and Selective Detection of Ricin Holotoxin," DARPA AMRI Review, New Orleans, LA, October 6, 2006.

J. Chen, J. Liu, M. Zhu, M. Yu, and W. Zhou, "ZnO One Dimesional Nanowire Synthesis and Nanodevices Fabrication by Nanolithography," DARPA AMRI Review, New Orleans, LA, July 13-14, 2006.

J. Liu, J.J. Chen, M. Zhu and W.L. Zhou, "Electric Properties Measurement of Mn Doped ZnO Aligned Nanoneedles Using Nanomanipulators in-situ FESEM," 2005 International Congress of Nanotechnology, San Francisco, CA, October 31- November 3, 2005.

Lesley Campbell A.D., Damon Smith, Garrett May, Yuxi Chen, Kevin Stokes, Weilie Zhou, "Nanolithographically Patterned Metal Oxide Nanowire Arrays for Highly Versatile and Sensitive Gas Sensors" International Congress of Nanotechnology, Oct.31-Nov.3, San Francisco, 2005